VTT Technical Research Centre of Finland

Urban low-to-medium deep borehole field regeneration with waste heat from energy efficient buildings: a techno-economic study in Nordic climate

Wallin, Andrei; Thomasson, Tomi; Abdurafikov, Rinat

Published in:
Energy and Buildings

DOI:
10.1016/j.enbuild.2023.113628

Published: 17/10/2023

Document Version
Publisher's final version

Energy & Buildings 300 (2023) 113628

Contents lists available at ScienceDirect

Energy & Buildings

journal homepage: www.elsevier.com/locate/enb

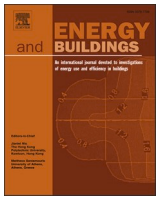

Urban low-to-medium deep borehole field regeneration with waste heat from energy efficient buildings: A techno-economic study in Nordic climate

Andrei Wallin, Tomi Thomasson *, Rinat Abdurafikov

VTT Technical Research Centre of Finland Ltd, Tekniikantie 21, 02150 Espoo, Finland

ARTICLE INFO

Keywords:
Shallow geothermal energy
Borehole heat exchangers
Waste heat
Regeneration
Techno-economic assessment

ABSTRACT

Due to large area requirement, ground-source heat pump (GSHP) systems with shallow boreholes are difficult to implement in dense urban areas. To address this limitation, alternative heat sources can be used to reduce heat extraction from ground or to inject regenerative heat to boreholes. This study investigates the techno-economic feasibility of utilizing two commonly available waste heat sources (waste air and wastewater) in urban environment. Passive and heat pump-assisted utilization are studied for apartment and office buildings, with varied borehole depth and two levels of urban density. Long-term GSHP system operation is simulated using iterative heat balance calculation and borehole dimensioning algorithms. The results show significant reduction in required borehole length with waste heat utilization, particularly in shallow borefields, with maximum reductions of 53.9% (apartment building) and 25.8% (office building). The studied waste heat sources are shown to enable a shallow borefield for otherwise insufficient borehole spacing, providing an alternative to deeper boreholes. However, waste heat only available during summer has limited impact on field sizing compared to a seasonally stable heat source. From an economic perspective, the levelized cost of heating could be reduced by 13.5% (apartment building) and 7.3% (office building) compared to baseline without waste heat utilization.

1. Introduction

The heating and cooling sector must contribute to the objective of carbon neutrality. Ground-source heat pumps (GSHPs) are a promising solution for achieving carbon neutrality in urban areas, with a projected significant increase in installed capacity. The global growth rate in installed capacity has followed a nearly exponential trend since the 1990s, with a growth rate of 11% in the previous decade [1]. The REPowerEU Plan states that the European Union member states can accelerate the deployment and integration of large-scale heat pumps, geothermal and solar thermal energy in a cost-effective way by, among other measures, clean communal heating, especially in densely populated areas and cities [2]. Outside of the EU, high growth estimates have been reported for China (28% capacity increase [3]) and Norway (ca. 16% growth rate [4]) for the current decade. Funding schemes for GSHP investments have also been made available in developing markets such as Germany and Spain [5]. In Finland, the utilization of GSHPs has evolved from small single-family home applications to larger installations in multi-family apartments and commercial buildings in the past decade [6].

Buildings with GSHPs require a certain amount of landmass to cover their annual energy needs sustainably for longer periods due to the decrease in ground temperature caused by heat extraction. However, the landmass may not be available in densely built urban areas. The limitation in area availability is further exacerbated by the minimum borehole spacing requirement – a minimum spacing of 5–8 m [7] has been suggested to minimize thermal interactions within borehole field. Consequently, shallow borehole fields may face challenges in meeting the energy demands of high-rise buildings. Various strategies have been proposed to address the limited availability of land for GSHPs. One possible solution is to increase depth of boreholes to access higher ground temperatures. However, deeper boreholes are generally considered to have greater geological uncertainties and technical drilling challenges, which can result in increased drilling costs [8]. Therefore, despite the existence of single deep boreholes [9,10] the widespread adoption of GSHPs with deep borehole fields has not yet been achieved commercially [6,11]. Another approach is to reduce net heat extraction from the ground by utilizing alternative heat sources, such as waste heat from industrial or commercial activities, solar energy, ambient air, waste air, or wastewater. The alternative heat sources can be used directly as heat sources for the heat pump, if the heat availability

* Corresponding author.
E-mail address: tomi.thomasson@vtt.fi (T. Thomasson).

https://doi.org/10.1016/j.enbuild.2023.113628
Received 10 July 2023; Received in revised form 27 September 2023; Accepted 9 October 2023
Available online 11 October 2023

Nomenclature

Acronyms

AB	apartment building
BHE	borehole heat exchanger
CAPEX	capital expenditure
COP	coefficient of performance
DHW	domestic hot water
EAHR	exhaust air heat recovery
GSHP	ground-source heat pump
HP	heat pump
HX	heat exchanger
LCOH	levelized cost of heating
MFT	mean fluid temperature
OB	office building
OPEX	operating expenditure
PV	photovoltaic
WA	waste air
WW	wastewater

Subscripts

cond	condenser
evap	evaporator
f	borehole fluid
m	borehole wall

Symbols

c	specific heat capacity ($Jkg^{-1}K^{-1}$)
H	Depth (m)
$\dot{m}$	mass flow rate (kgs^{-1})
q	specific heat extraction rate (Wm^{-1})
Q	heat flow rate (W)
r	specific enthalpy of condensation (Jkg^{-1})
R	thermal resistance (m^2KW^{-1})
T	Temperature (K)
$\dot{v}$	volumetric flow rate (m^3s^{-1})
x	absolute humidity (gkg^{-1})
ε	heat exchanger effectiveness (–)

matches temporally with the heat demand, or to regenerate the ground by injecting heat to boreholes.

Several studies have investigated the utilization of waste heat from commercial or industrial activities. Li et al. [12] conducted a study on the utilization of data center waste heat in a shallow (240 × 55 m) borehole thermal energy storage field in Norway. With the field, a 15% lower peak load and an 83% reduction in dissipated waste heat were achieved compared to a district heating system connection. Guo et al. [13] investigated the use of waste heat from cooling process of a copper plant in China. With shallow borehole heat exchangers (BHE) (400–800 × 80 m) and an absorption heat pump, a 28.8% reduction in fossil energy demand was achieved. In Norway, the KIWI Dalgård supermarket [14] utilized a shallow borehole field (8 × 264 m) to store the excess heat from the refrigeration system. Despite the borehole system being undersized, the results indicated balanced heat extraction and supply. Solar energy and ambient air regeneration are highly dependent on latitude, and therefore may be only seasonally available. Hemmatabady et al. [15] developed a combined multi-objective optimization and simulation model and studied heating and cooling operation of solar thermal collectors, air-source heat pump and a shallow borehole field in a context of an urban quarter in Germany. Hirvonen & Siren [16] studied a system based on solar PV coupled with heat pumps, water tanks as well as a borehole thermal energy storage to cover thermal loads of a community with hundred low energy residential buildings in Finland. Based on a preceding study by the same authors [17] it was suggested that the integration of solar thermal collectors results in about 36% higher lifecycle cost compared to the solar electric configuration. Allaerts et al. [18] studied utilization of ambient air to adjust the heat balance of two shallow (130 m) borehole fields – one dedicated for heating and another primarily for cooling of an office building in Belgium. The solution based on ambient air regeneration enabled a 47% lower borehole field size and 37% lower installation cost compared to a stand-alone GSHP system. Next, the utilization of waste heat from space cooling for borehole regeneration has been explored at varied levels. Walch et al. [19] studied shallow boreholes (50–300 m) in a regional area in Switzerland. Seasonal regeneration with space cooling was found to increase the heat extraction potential per ground area significantly in urban areas from 15 kWh/m^2 to 330 kWh/m^2. Puttige et al. [20] studied the optimal use of a GSHP system (125 × 200/250 m) in a hospital in Sweden. While the benefit of regeneration was not explicitly studied, four operating modes for the GSHP were considered, including active cooling and active cooling with free cooling. Although the average cooling degree days values have increased in the EU over the last decades, the space cooling demand in the Nordic countries is relatively low [21], leading to a low overall ground regeneration potential.

Considering wastewater and waste air, the former is a typically seasonally stable source of heat that is available in all residential buildings. Particularly in new buildings, wastewater heat loss can account for a significant portion of total heat loss. This heat can be recovered directly at the point of consumption such as shower or dishwasher, or by using a centralized heat exchanger typically located in the basement of a building. By using a centralized heat exchanger, it is possible to utilize the recovered heat for heating the ground loop, thereby reducing the net heat extraction from ground. The exhaust air from buildings without exhaust air heat recovery system provides a stable source of heat throughout the year. Since exhaust air constitutes a significant portion of a building's heat losses, exhaust air heat recovery is widely implemented in Northern and Central Europe [22], and for example, in Finland, has been mandatory for new buildings in Finland since 2003 [23]. These systems, usually implemented as part of air handling units, transfer heat from extract air into supply air streams during heating season. However, during summer and partially during spring and fall, the exhaust air bypassing or after the heat exchanger is still warm enough for direct thermal regeneration of ground boreholes. Exhaust air heat pumps are increasingly used to harness this potential and can be used in combination with a GSHP or district heating system to augment the energy supply. In Finland, Hirvonen et al. [24] studied a mid-sized apartment building with a shallow GSHP system (10 × 100 m) and without ventilation heat recovery. A combination of exhaust air (55%) and wastewater (45%) for regenerating a ground loop led to a 20% lower life cycle cost than relying solely on a traditional borehole field without additional energy sources. Moholt 50|50 [14], a student village in Norway, implemented a shallow GSHP system (23 × 250 m) with three sources for borehole charging, namely solar thermal (12%), heat recovery from gray water (50%), and ventilation air (38%). Although solar thermal was found to be economically infeasible, heat recovery from ventilation air was considered to induce low additional costs. Heat recovery from wastewater enabled low costs (6c/kWh_{th}), provided sufficient wastewater quantities are available.

1.1. Contribution of this study

In literature, the benefits of waste heat utilization in conjunction with GSHPs have been explored in relation to different building types, waste heat sources, and electricity price assumptions. However, the reviewed studies primarily focused on shallow (<300 m) boreholes, and

mainly evaluated a single predefined field configuration. A comprehensive analysis that combines various field depths and quantifies the benefits of both passive (direct) and active (heat pump assisted) waste heat utilization for GSHP systems in different building types has not been carried out. To fill the research gap, we conduct a techno-economic analysis of GSHP systems in two example buildings – an office building and an apartment building – situated on a limited plot of land. We consider different combinations of borehole field depth and waste heat options – wastewater, waste air (exhaust air after heat recovery), or both – and evaluate the optimal dimensioning and long-term techno-economic performance for each combination using a developed dimensioning algorithm and system model. Specifically, we focus on comparing the cost-effectiveness of increasing borehole depth versus introducing waste heat sources to cover building heat demand or to regenerate the borehole field. To assess the benefits of the waste heat recovery, we use a configuration without waste heat utilization, and a district heating and cooling connection as the benchmarks.

2. Materials and methods

2.1. Studied buildings

The study selected an apartment building and an office building as case buildings. Both buildings are modern and meet minimum mandatory energy efficiency requirements. The office building, located in Espoo, Finland, was commissioned in 2020. The apartment building, located in Helsinki, Finland, is expected to be commissioned in 2023. The heating and cooling loads of the buildings were obtained using building energy simulation in IDA-ICE [25], with test reference year 2012 for Vantaa as climate data [26]. The land area available for boreholes was obtained from building net area and a floor area ratio of 2.5, selected to represent a typical new dense apartment building districts in Helsinki. The floor area ratio here relates floor area of buildings to area of land plot and parts of adjacent public areas such as sidewalks and streets. To investigate the impact of the floor area ratio, a case with smaller buildings was formulated: the available land surface area remains the same, but the heating and cooling loads of the buildings were scaled down using a factor of 0.5. In this case, specific thermal loads of buildings per unit of floor area remain unchanged while the floor area ratio becomes 1.25, reflecting districts with larger plots and lower-rise buildings more typical for districts of moderate urban density [27]. Table 1 summarizes the main technical parameters and energy consumption values of the buildings. In addition, the heating and cooling loads of the apartment and office buildings are shown in Fig. 1. The office building has higher ventilation flow rates, resulting in higher annual demand for ventilation heating and cooling, as well as significantly higher peak loads. Moreover, in the office building, ventilation flow rates are controlled according to office hours, which introduces cyclicity to heating and cooling loads.

In both buildings, the heating and cooling supply system is built around ground-source heat pumps (HP) that fully cover the heating and cooling loads of the building. The system is designed for Nordic climate conditions, with the focus on covering the heating demand, and minimizing the waste heat flows. Mechanical supply and exhaust ventilation systems of the buildings incorporate high-efficiency exhaust air heat recovery (EAHR), which can reduce exhaust air temperature to a minimum of 0 °C, especially in winter, depending on outdoor temperature. Additional heat recovery exchanger is placed in the exhaust air stream after the EAHR device. The schematic layout of the studied system is presented in Fig. 2. Although the layout shows a single HP, in practice, several may be installed. The layout enables the use of heat recovered from wastewater (HX2) and exhaust air (HX3) to either directly regenerate the ground loop (passive connection) or to feed as a heat source for HP (active connection). In the latter case, heat exchangers HX2 and HX3 are connected to a cooling loop, circulated by the pump P2. The wastewater heat exchanger HX2 is only present in the apartment building. Heat input to the HP is controlled by valves V1 and V2 and collected from either the ground loop circulated by pump P1, or the cooling loop, or both. The cooling loop has a priority to enable higher utilization of the waste heat. If heat input from the cooling loop is inadequate, additional heat from the ground loop is directed to HP evaporator. Valve V4 is used to alternate the heat output of HP to space and ventilation heating loads or DHW. Active borehole regeneration takes place when energy from cooling and waste heat sources (upgraded to HP condenser side) exceeds the heating loads of the building. In this case, the surplus is transferred to the ground loop via valve V3 and heat exchanger HX1. HX1 is also present in the passive connection, since the cooling loads during summer can exceed heating loads, in which case the surplus heat needs to be transferred to the ground loop.

Table 1
Building parameters, simulated annual energy and peak loads of heating and cooling.

Parameter	Unit	Apartment building (AB)	Office building (OB)
Building net area	m^2	7400	7900
Building roof area	m^2	850	1150
Building plot area	m^2	2960	3160
Heating temperature setpoint	°C	21	22
Cooling temperature setpoint	°C	26	25
DHW supply temperature	°C	58	
Space and ventilation heating supply temperature	°C	20–40	
Space and ventilation cooling supply temperature	°C	9	
Ventilation heat recovery efficiency	%	82	
Ventilation daily operating hours	h	24	11 (07:00–18:00)
Ventilation flow rate during operating hours	$l/s/m^2$	0.5	2.0*
PV capacity	kW_p	57	77
Annual space and ventilation heating demand	kWh/m^2 (W/m^2)	15.9 (21.0)	29.0 (48.2)
Annual space and ventilation cooling demand	kWh/m^2 (W/m^2)	4.5 (17.3)	11.2 (47.2)
Annual domestic hot water demand	kWh/m^2 (W/m^2)	41.3 (10.3)	10.1 (2.6)
Number of residents (for wastewater calculation)		230	–

* 0.15 $l/s/m^2$ outside operating hours.

2.2. Waste heat calculation

Waste air and wastewater were selected as the waste heat sources for the study, as they are available in most buildings. These energy sources also differ in their temporal availability, with wastewater energy being more stable throughout the year, while waste air energy is mostly available during summer. Heat exchangers transferring heat from the waste heat sources were modelled based on heat exchanger effectiveness ε (Eq. (1)). In the equation, the heat source side is represented by either waste air or wastewater, while the heat sink side is represented by ground loop or cooling loop temperature.

$$\varepsilon = \frac{Q}{Q_{max}} = \frac{Q}{\min(\dot{m}_{sink},\ \dot{m}_{source}) \times c_p \times (T_{source,in} - T_{sink,in})} \quad (1)$$

The wastewater of the apartment building is assumed to pass through

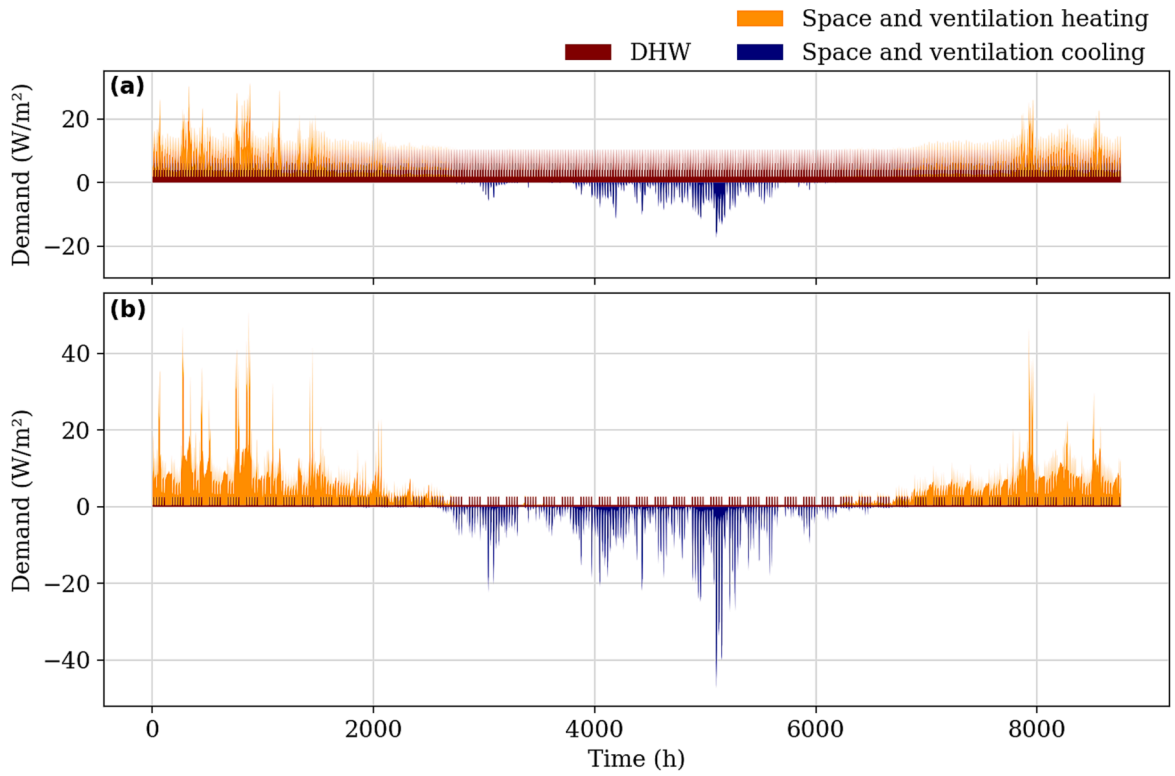

Fig. 1. Load profiles of the apartment (a) and office (b) buildings. The heating loads are shown as stacked space heating and domestic hot water loads. Cooling loads are shown as negative values.

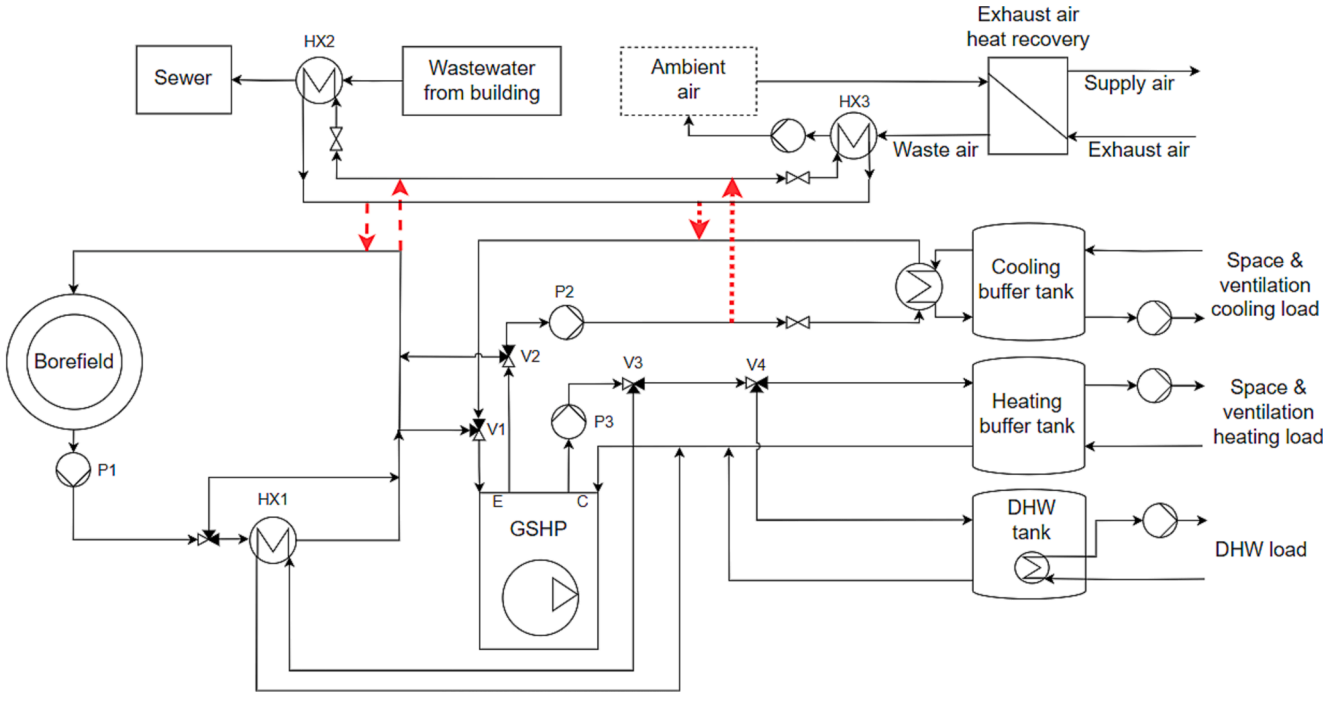

Fig. 2. Schematic of the studied building energy system. The connections enabling passive and active waste heat utilization are highlighted with dashed and dotted lines respectively.

a heat exchanger located in the basement. The heat sink flow rate is directly determined from the ground loop or from the cooling loop, and the wastewater outlet temperature is limited to 5 °C. A constant value of 0.45 for heat exchanger effectiveness was used based on manufacturer data of a commercial wastewater heat exchanger [28]. Similar effectiveness values have been measured from various types of wastewater heat recovery systems [29]. Wastewater flow and temperature profiles used in the apartment building simulation were generated based on the results of a previous study [30], where a wastewater generation model introduced in [31] was improved to account for in-building

cooling and to better match water consumption patterns in Finnish cities. The used profiles consider seasonal and diurnal variation in temperature, and diurnal variation of flow rate, while the daily amount of wastewater is assumed constant at 110 l/resident/day. Wastewater temperature before the heat exchanger depends on the season due to varying temperature of in-building sewer pipes and cold water supply, and on flow rates, as lower flow has lower heat capacity. Shower use, which accounts for most of the hot water consumption in the buildings, is associated with high flow rates.

In this study, waste air is used to refer to exhaust air after the EAHR to supply air, to differentiate between exhaust air before and after heat recovery, since there is a considerable difference in the energy potential between the former and latter. For waste air heat exchanger, a constant effectiveness value of 0.7 was used based on previous experience with similar systems. The temperature of the waste air after EAHR varies from 0 °C in winter to around 26 °C in summer, in a modern building with cooling. Compared to ambient air, waste air temperature is consistently high during summer, while ambient air temperature rarely exceeds 25 °C and often drops to 10–15 °C at night. Time series for waste air temperatures and flow rates were obtained from the IDA-ICE simulation. To prevent frost formation, the minimum outlet temperature from the waste air heat exchanger was selected to be 0 °C. During most of the winter, the waste air temperature is already at 0 °C after EAHR and therefore no further recoverable energy is available during most of the winter. Condensation of air moisture also contributes to heat recovery from waste air. The condensation heat $Q_{\text{condensation}}$ was calculated using (Eq. (2)) from air mass flow rate ($\dot{m}$), specific enthalpy of condensation (r) and the change in absolute humidity Δx. The change in absolute humidity was calculated using (Eq. (3)), in which the heat exchanger surface temperature T_{surf} was assumed as an average between the heat sink and heat source inlet temperatures.

$$Q_{\text{condensation}} = \Delta x \times \dot{m} \times r \tag{2}$$

$$\Delta x = (x_{\text{in}} - x_{\text{surf}}) \times \frac{(T_{\text{in}} - T_{\text{out}})}{(T_{\text{in}} - T_{\text{surf}})} \tag{3}$$

Fig. 3 shows the available energy from wastewater and waste air the apartment building and waste air in the office building in hourly resolution when the flows of heat sources are cooled down to their minimum temperature limits. The estimated annual recoverable heat from waste air was greater for the office building (117.8 kWh/m^2) than for the apartment building (83.6 kWh/m^2). Also, the peak values were higher for the office building, due to high air flow rates during hours of occupancy. The amount of heat recoverable from wastewater in the apartment building annually was 23.9 kWh/m^2. Due to unavailability of typical office building wastewater profiles for this study, an estimate based on Finnish guidelines for building energy calculation [32] suggests that the DHW consumption of an office building is around six times smaller than that of apartment building. A similar ratio can be expected for recoverable wastewater energy, rendering wastewater heat recovery unlikely to be profitable. In the results section, we use utilization rate, defined as the percentage of utilized waste heat energy to the theoretically recoverable waste heat energy presented here, to investigate the portion of waste heat energy that is practically usable in each scenario. In addition, we use matching rate, defined as the percentage of waste heat that on the hourly level coincides with heat demand.

2.3. System model

For borefield simulation, an open-source Python library, pygfunction [33], was used to calculate field thermal response functions, also known as g-functions. The g-function relates the average borehole wall temperature change of a field to a constant net heat extraction with a specific duration. Uniform borehole wall temperature was used as boundary condition for calculating the g-functions, which were used in conjunction with the convolution method [34] to obtain the hourly time series of average borehole wall temperatures, based on a given hourly time series of borehole net heat load. The temperature of fluid circulating in the ground loop was calculated from average borehole wall temperatures using a model of BHE. For U-tube BHEs, a simplified approach was employed, as first introduced by [35], where the BHE is modelled using an effective resistance value R_{b}. This value, along with heat extraction rate $\overline{q}$, and their relation (Eq. (4)) was used to solve the mean fluid temperature (MFT) in the borehole $\overline{T}_{\text{f}}$, further allowing the inlet and outlet fluid temperatures to be estimated from the mean temperature assuming symmetry (Eq. (5)). In the coaxial BHE, fluid inlet and outlet temperatures were calculated using an analytical borehole model described in [36] which determines fluid temperature profiles along the BHE from input of ground temperature gradient and heat extraction rate. However, uniform (with respect to depth) ground temperature was used as input for this model as well.

$$\overline{q} = \frac{\overline{T}_{\text{f}} - \overline{T}_{\text{b}}}{R_{\text{b}}} \tag{4}$$

$$\overline{T}_{\text{f}} = \frac{T_{\text{in}} + T_{\text{out}}}{2} \tag{5}$$

The used modelling approach necessitates substituting depth-varying temperatures with an average value. As g-functions represent the average borehole wall temperature change, no information about

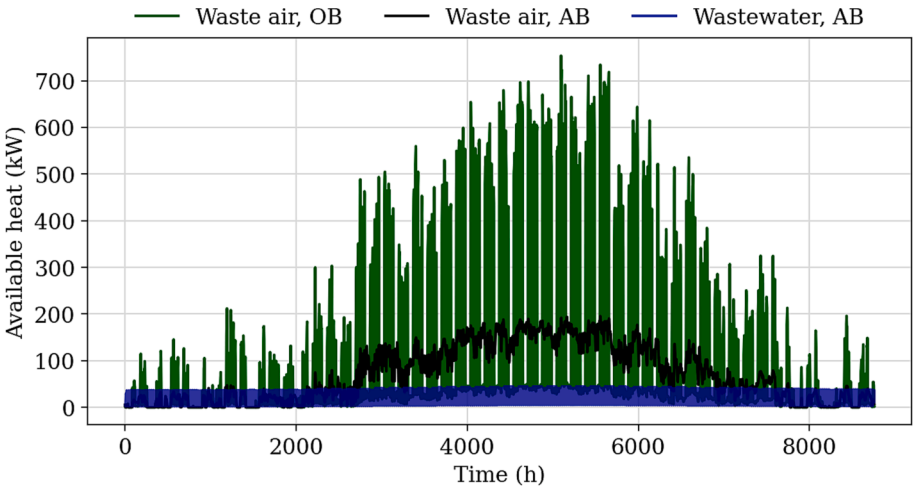

Fig. 3. Calculated hourly theoretically available energy from waste air and wastewater, for the office (OB) and apartment (AB) buildings.

the vertical borehole wall temperature gradient is acquired regardless of the boundary condition. Alternative analytical approaches, such as a segmented finite cylinder-source model [37], have been shown to enable the description of depth-varying temperature profiles, but may introduce constraints related to computation time. The assumption of average temperature is inherently more accurate for shallow boreholes, where the difference in ground temperatures between the top and bottom of the borehole is smaller. Since the study includes deeper boreholes, the used modelling approach was validated against a numerical borehole heat exchanger model to ensure its accuracy.

The overall calculation procedure for the ground heat balance is illustrated in Fig. 4. An iterative algorithm was used, since the ground loop temperature calculation is based on net heat extraction from ground, and net heat extraction is in turn affected by the operation of waste heat exchangers and HP with dynamic coefficient of performance (COP). The utilizable waste heat (Eq. (1)) and HP performance can be calculated after solving the ground loop fluid temperatures as described above. For the HP COP, Eq. (6) was used based on measurement data of a commercial HP. Flow pressure loss (Δp) in the BHE flow channels was calculated from the Darcy friction factor. Circulation pump power was calculated from the pressure loss and volumetric flow rate ($\dot{v}$) in (Eq. (7)). For calculating the pumping power, the pressure losses in waste heat exchangers and the HP were assumed negligible compared to the pressure loss in the BHEs.

$$\mathrm{COP} = -0.0752 \times T_{\mathrm{cond}} + 0.0675 \times T_{\mathrm{evap}} + 7.4174 \tag{6}$$

$$P = \frac{\dot{v} \times \Delta p}{\eta} \tag{7}$$

Since the required number and depth of boreholes were subject to change in field dimensioning, iterative algorithms were developed to automate this task, iterating over borehole count, depth, or both. Circular borehole arrangement with boreholes placed at equal distances on the circumference of a circle was exclusively used, since it allows for simpler dimensioning algorithms with an arbitrary number of boreholes. For most other field shapes, the effect of reducing the borehole count depends on which borehole is removed, requiring separate analysis for each borehole. In thermal perspective, the circular borehole arrangement has an advantage of excluding the boreholes in the center of the field, which tend to be weakest in terms of performance [38]. To ensure the comparability of the performance of field configurations at different depths, the same dimensioning criteria were used for all cases. Specifically, the minimum borehole mean fluid temperature (MFT) over 50 years of operation was required to remain above 0 °C.

2.4. Scenarios and techno-economic assumptions

To evaluate the benefits of waste heat utilization, the study examined both active and passive utilization of wastewater and waste air energy sources, as well as their combination, resulting in a total of six scenarios for the apartment building. For the office building, the wastewater resource was assumed to be negligible, and therefore only two scenarios (passive and active waste air) were considered. For both building types, a baseline scenario without waste heat utilization was included. All the

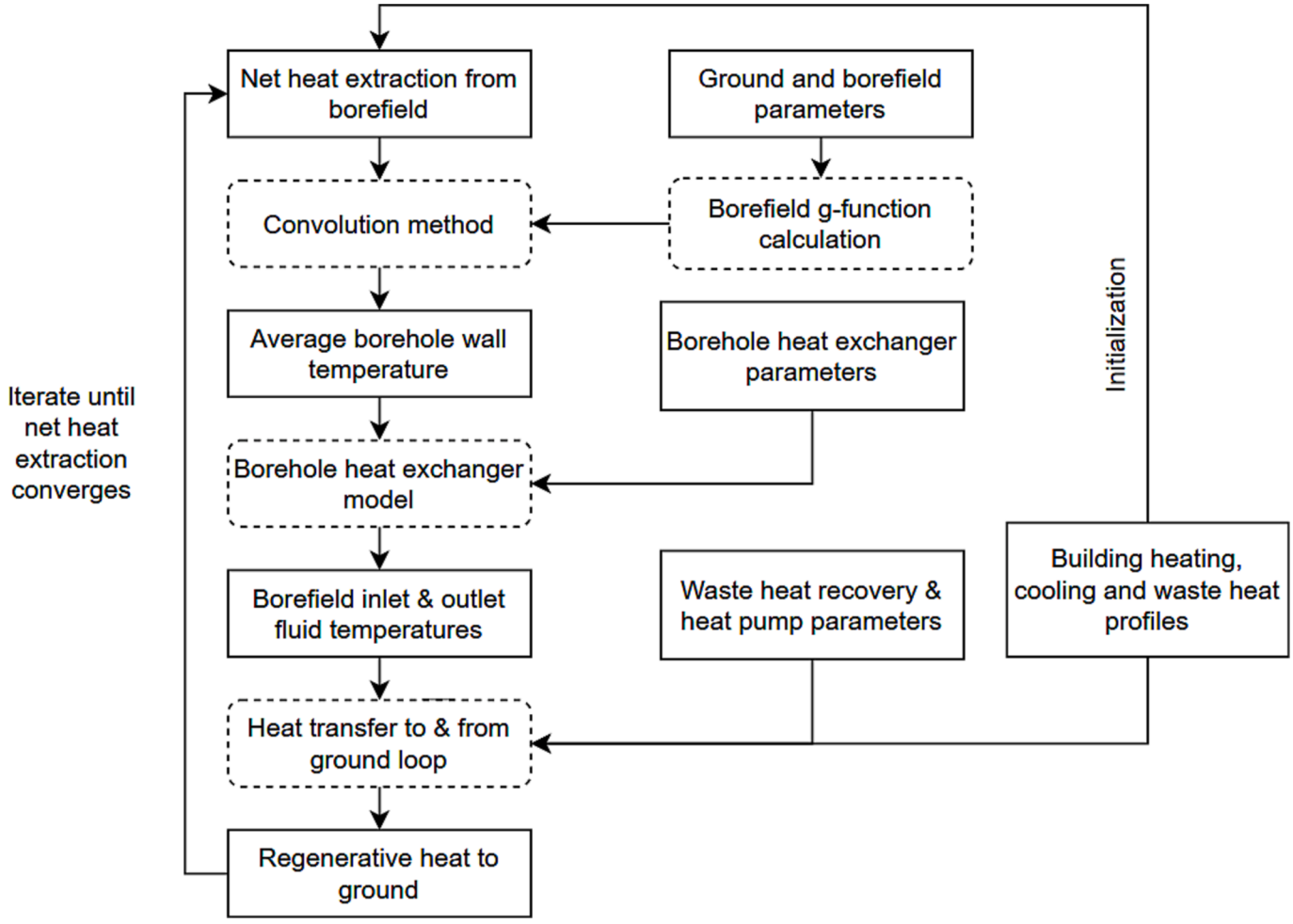

Fig. 4. Procedure for calculating ground heat balance including borehole regeneration.

scenarios were calculated for both building sizes, representing the two different levels of urban density with floor area ratios of 2.5 and 1.25. Table 2 summarizes the studied scenarios and the used acronyms in the results and discussion section.

The study included three depth classes of 300 m, 500 m, and 800 m to represent shallow, intermediate, and semi-deep boreholes, respectively, for each scenario. In baseline scenarios of each depth class, the dimensioning algorithm was used to generate a circular field with largest possible radius fitting the square-shaped plot area. Since both borehole MFT (the dimensioning criteria) and depth cannot be strictly enforced without altering other parameters, such as load coverage, the borehole depth was considered a soft target. In practice, technical or legislative reasons may exist to prioritize reduction of depth, but in this study, no depth restrictions were assumed and minimizing the borehole count for each configuration was assumed as the main target, expectedly enabling the highest benefit in saved drilling time and cost. The algorithm determined the field configuration closest to the depth target while still satisfying the minimum MFT requirement during system lifetime of 50 years. Based on the baseline scenario, the effect of waste heat utilization on borehole field dimensioning was assessed in other scenarios. First, the number of boreholes was reduced, if the decrease of required total borehole length was high enough, and when no more boreholes could be eliminated, the depth of the remaining boreholes was decreased. Reducing the number of boreholes was prioritized over decreasing field depth as it allows for increased spacing between the remaining boreholes, thereby enhancing their performance. In passive scenarios, all available waste heat energy was transferred to the ground loop, and in active scenarios the amount of utilized energy was limited from above to a value corresponding to net ground zero heat balance (annual heat injection equals heat extraction), since using electricity to increase the field long-term temperatures was not deemed beneficial. Minimum temperature of the cooling loop flow to waste heat exchangers was assumed as −5 °C, which was another limiting factor for the active scenarios. From thermal perspective, a universal lower limit for borehole spacing is not definable since the annual net heat extraction of each individual borehole determines the extent of ground cooling around the borehole. However, there are practical concerns related to drilling adjacent boreholes with inadequate spacing. Drilled boreholes are not geometrically straight nor vertical lines, and their inclination can be difficult to control [39,40], which increases the risk of borehole collision. In this study, 8 m was chosen as a safety limit for spacing, and scenarios not fulfilling the spacing limit were marked in the results to highlight the possibility of utilizing regeneration to increase the borehole spacing above the safety limit.

Different technical parameter assumptions were made depending on the borehole depth class. Borehole flow rate was assumed to increase with borehole depth to minimize shunt heat transfer between upward and downward traveling fluids [41]. Borehole diameter was also scaled with depth to limit pressure loss with higher flow rates. For the shallow and intermediate depth classes, a U-type BHE was assumed, while a coaxial BHE was assumed for the semi-deep depth class, as the latter geometry enables lower pressure loss for a given flow rate compared to U-tube [41]. The tube diameter and thickness of the U-tube borehole between the shallow and intermediate BHEs were also adjusted due to the increase of flow rate. The flow rate in each type of borehole was controlled within a given range, changing in linear proportion to heat extraction from or heat injection to the ground loop, whichever is larger at the given time step. For the coaxial BHE, the fluid flow was input from the annulus. Technical parameters related to boreholes, and ground properties are summarized in Table 3.

Table 4 summarizes the economic parameter assumptions of the study. Constant electricity price was conservatively assumed due to increased uncertainty experienced in Nordic electricity prices during recent years. For the borehole heat exchanger, the specific investment cost is assumed to increase gradually with depth due to increased drilling cost, leading to a higher cost level with deeper fields in comparison to reference studies (e.g., 40 €/m, [42]; 33.5 €/m [43]). The cost levels were selected to reflect price estimations of Finnish projects. Similar gradual increase is also applied by, for example, Mazzotti et al. [39], who presented a survey-based price model of borehole drilling cost as a function of depth, with the borehole cost per meter increase described by a quadratic price model. Wastewater heat recovery heat exchanger costs were estimated based on commercial products [28,44] deemed suitable for the large and small apartment building, respectively. An installation cost of 30% of the large-scale heat exchanger's cost was used for both building sizes. For waste air heat recovery heat exchangers, the cost estimate basis was an expert estimate of 10 k€ including installation, when the heat exchanger is installed as an additional module in the ventilation unit for the large apartment building. Equipment and installation costs for the waste air heat exchanger were each assumed to cover half of the total cost and were scaled between the buildings based on the "0.6 rule" [45] with factors of 0.6 and 0.5, respectively, based on building peak ventilation flow rates. Finally, a configuration with district heating and cooling connection was formulated to compare the

Table 2
Studied scenarios and the selected regeneration energy sources.

	Apartment building (AB)		Office building (OB)	
	Active	**Passive**	**Active**	**Passive**
Wastewater (WW)	WWA	WWP	–	–
Waste air (WA)	WAA	WAP	WAA	WAP
Combined	COMA	COMP	–	–
None	BASE		BASE	

Table 3
Technical borehole heat exchanger of the studied depth classes and ground properties used in the study.

Depth class	**Shallow (300 m)**	**Intermediate (500 m)**	**Semi-deep (800 m)**
Common parameters			
BHE type	U-tube	U-tube	Coaxial
Borehole diameter (mm)	110	140	155
Flow rate per borehole (kgs^{-1})	0.3–0.6	0.5–1.0	1.1–2.2
Circulation fluid	Kilfrost, 30 vol-%		
Circulation pump electrical efficiency (%)	65		
U-tube parameters			
Tube thickness (mm)	4	5	–
Tube outer diameter (mm)	40	50	–
Tube shank spacing (mm)	75	75	–
Tube thermal conductivity ($Wm^{-1}K^{-1}$)	0.3	0.3	–
Coaxial parameters			
Inner tube thickness (mm)	–	–	5
Inner tube outer diameter (mm)	–	–	70
Inner tube thermal conductivity ($Wm^{-1}K^{-1}$)	–	–	0.15
Outer tube thermal conductivity ($Wm^{-1}K^{-1}$)	–	–	0.3
Outer tube thickness (mm)	–	–	5
Ground parameters			
Ground surface temperature (°C)	7.0		
Ground geothermal gradient (°C/100 m)	1.3		
Ground conductivity ($Wm^{-1}K^{-1}$)	3.15		
Ground density (kgm^{-3})	2640		
Ground heat capacity ($Jkg^{-1}K^{-1}$)	720		

Table 4
Default economic parameter values used in the study.

Parameter	Value	
General		
Reference electricity price (incl. transmission)	15	c/kWh
District heating scenario		
District heating energy fee	10.67	c/kWh
District heating water flow fee	0.93	€/h
District cooling energy fee	5	c/kWh
Investment costs		
Weighted average cost of capital	6	%
Borehole heat exchanger	*H*/10	€/m
Heat pump	800	€/kW_{th}
Solar PV	700	€/kW_{p}
Electric boiler	75	€/kW_{th}
Wastewater heat exchanger (AB, large/small)	40.9/38.3	k€
Waste air heat exchanger (AB, large/small)	10.0/7.0	k€
Waste air heat exchanger (OB, large/small)	23.4/14.7	k€

economic performance of the GSHP systems with more traditional supply systems. The cost data was retrieved from the local district heating company [46] using price information from 2022. The total annual cost, consisting of energy fee for heating and cooling, water flow fee, and annualized investment cost, were calculated based on the heating and cooling demand.

3. Results and discussion

3.1. Model validation

The developed iterative model for calculating the ground heat balance was validated against a BHE model implemented in dynamic simulation software Apros [47] to show that the presented model, which includes simplified temperature handling and ignores dynamic effects in the BHE, leads to results comparable to a numerical model. In the numerical BHE model, previously presented in [36], the whole system including regeneration heat transfer is solved dynamically at each timestep. Technically, the aim of the validation was to evaluate the accuracy of the iterative model in calculating the regeneration heat transferred to ground and its subsequent effect on fluid temperatures, especially in transient situations. In the validation, a single BHE was simulated for one year, using a dynamic HP COP (Eq. (6) and passive WA regeneration. A semi-deep BHE with parameters according to Table 3 was selected to include the highest possible inaccuracy caused by the average ground temperature assumption of the developed model, as discussed in Section 2.3. Fig. 5 displays ground net heat and MFT for a selected week during summer, with simultaneous DHW and cooling load, and regeneration. Despite the simplified handling of ground and borehole wall temperatures in the developed model, the mean absolute error of MFT over the entire year was 0.27 °C, indicating a good level of agreement. The most significant errors occurred during load changes, where the developed model tended to overestimate changes in fluid temperature. This behavior is common in models based on long-term g-functions, which do not consider the heat capacity within the BHE, as discussed in previous studies such as [34]. The difference in MFT at the time of annual minimum of MFT was 1.51 °C, meaning that the studied approach leads to slightly over-dimensioned fields. However, this was considered an acceptable safety margin. Furthermore, the absolute error in annual regeneration heat was 0.62 MWh, which amounted to 1.7% of the total regeneration heat of 35.9 MWh.

3.2. Scenario overview

Table 5 presents the borehole count, depth, total borehole length, and borehole spacing for all the simulated scenarios defined in Table 2, resulting in 60 different borefield configurations. Borefields that fail to meet the minimum borehole spacing requirement of 8 m are shown with an asterisk. It was observed that the baseline scenarios with the shallow fields and large buildings (dense urban development) did not satisfy this requirement. However, for the AB, the minimum spacing could be achieved with active and combined waste heat utilization. In the case of the OB, WA utilization did not lead to a sufficient reduction in the borehole count, resulting in too narrow borehole spacing, even with zero heat balance with ground. All the configurations of Table 2 are in circular arrangement, as introduced in Section 2.3. For borefield fields of different shapes, the exact results will differ. However, the same principle is applicable: by introducing regenerative heat, the borehole count can be reduced. Furthermore, if the field shape is tightly packed, involving weak boreholes situated in the middle of the field with many neighboring boreholes, the effect of regeneration is higher, since the energy output of weak boreholes is lower and therefore more easily substituted.

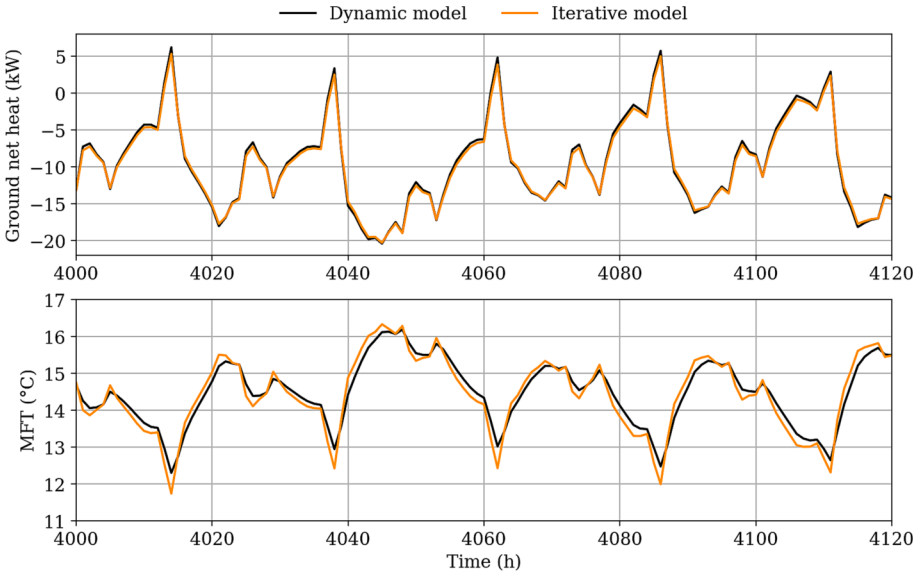

Fig. 5. Comparison of the results of the developed iterative model and a dynamic model, showing net heat extraction from ground (top) and mean fluid temperature inside borehole (bottom), for five days during summer.

Table 5
Dimensions of all calculated fields. The values are presented in the format "borehole count × borehole depth = total length (borehole spacing)". The field configurations not meeting the minimum spacing requirement of 8 m are shown with an asterisk (*).

Floor area ratio		2.5 (high urban density)		1.25 (moderate urban density)	
Depth class	**Scenario**	**AB**	**OB**	**AB**	**OB**
Shallow (300 m)	BASE	*34 × 300 = 10,200 (5.0)	*44 × 300 = 13,200 (4.0)	12 × 300 = 3600 (14.2)	19 × 297 = 5643 (9.3)
	WWP	*24 × 294 = 7056 (7.1)	–	10 × 288 = 2880 (17.1)	–
	WWA	20 × 291 = 5880 (8.5)	–	9 × 288 = 2592 (19.0)	–
	WAP	*22 × 294 = 6468 (7.8)	*33 × 297 = 9801 (5.4)	10 × 300 = 3000 (17.1)	17 × 291 = 4947 (9.3)
	WAA	19 × 288 = 5472 (9.0)	*33 × 297 = 9801 (5.4)	10 × 278 = 2780 (17.1)	17 × 291 = 4947 (9.3)
	COMP	17 × 297 = 5049 (10.0)	–	9 × 275 = 2475 (19.0)	–
	COMA	16 × 294 = 4704 (10.0)	–	8 × 297 = 2376 (21.4)	–
Intermediate (500 m)	BASE	12 × 500 = 6000 (14.2)	18 × 503 = 9054 (9.8)	5 × 513 = 2565 (34.2)	8 × 519 = 4152 (22.1)
	WWP	10 × 478 = 4780 (17.1)	–	5 × 444 = 2220 (34.2)	–
	WWA	9 × 472 = 4248 (19.0)	–	4 × 494 = 1976 (42.7)	–
	WAP	10 × 497 = 4970 (17.1)	16 × 491 = 7856 (11.0)	5 × 479 = 2395 (34.2)	8 × 491 = 3928 (22.1)
	WAA	9 × 491 = 4419 (19.0)	16 × 491 = 7856 (11.0)	5 × 450 = 2250 (34.2)	8 × 491 = 3928 (22.1)
	COMP	9 × 459 = 4131 (19.0)	–	4 × 494 = 1976 (42.7)	–
	COMA	8 × 478 = 3824 (21.4)	–	4 × 479 = 1916 (42.7)	–
Semi-deep (800 m)	BASE	5 × 800 = 4000 (34.2)	8 × 794 = 6352 (22.1)	2 × 906 = 1812 (85.5)	4 × 775 = 3100 (44.2)
	WWP	5 × 700 = 3500 (34.2)	–	2 × 794 = 1588 (85.5)	–
	WWA	4 × 765 = 3060 (42.7)	–	2 × 750 = 1500 (85.5)	–
	WAP	5 × 750 = 3750 (34.2)	8 × 757 = 6056 (22.1)	2 × 875 = 1750 (85.5)	4 × 750 = 3000 (44.2)
	WAA	5 × 694 = 3470 (34.2)	8 × 744 = 5952 (22.1)	2 × 831 = 1662 (85.5)	4 × 744 = 2976 (44.2)
	COMP	4 × 775 = 3100 (42.7)	–	2 × 762 = 1524 (85.5)	–
	COMA	4 × 735 = 2940 (42.7)	–	2 × 737 = 1474 (85.5)	–

Shallower fields in all the scenarios necessitate a higher total borehole length compared to deeper fields. This disparity arises because of smaller borehole spacings in shallow fields, resulting in increased thermal interference between boreholes. The performance of deeper fields is also improved by higher ground temperatures, for example, an average temperature of 9.0 °C for the shallow field and 12.2 °C for the semi-deep field, which effectively means that the deeper fields have a higher reserve of heat available. Consequently, individual boreholes in shallower fields perform less efficiently in terms of peak ground heat extraction rate and total net ground heat extraction per borehole meter, as illustrated in Fig. 6, when compared to deeper fields. At the same time, the maximum total borehole length reduction achieved with waste heat utilization is greater with shallow fields. Similarly, for the building versions with lower floor area ratio, the achieved borehole length reduction is lower since the fields are less dense.

Higher values of specific peak heat extraction rate can generally be observed for the OB compared to the AB (Fig. 6). On the contrary, in terms of specific annual net heat extraction, the AB typically exhibits greatly higher values in comparison to the OB. In this case, the field dimensioning of the OB is dictated by the peak heat demand, and energy-wise, the field is underutilized, as well as having higher total borehole length in absolute terms. The dependency of dimensioning alternatively on peak heat or energy also determines the effectiveness of seasonal waste heat utilization. For example, for the OB, active WA has relatively lower impact on dimensioning compared to the AB. This disparity arises because the dimensioning in the OB is primarily driven by the peak heat demand, and WA is not available to reduce ground cooling during the heating season.

3.3. Utilization and matching of waste heat

Annually utilized waste heat differs greatly by scenario. Less energy is utilized from WW than WA, in both passive and active scenarios, but the difference is not as large as suggested by theoretical available energy (Section 2.2), since utilization rate of WW is higher (Table 6). The active connection increases the utilization for both WW and WA. Active WA scenarios for the AB reach net zero ground heat balance, preventing further increase of utilization. With OB, net zero ground heat balance is reached for shallow and intermediate fields already with passive WA, and therefore little to no further improvement is achieved with active WA. The utilization rate of WA for OB is much lower than for the AB. This indicates potential for utilizing the heat of waste air from office buildings for other purposes, for example, regenerating fields of adjacent apartment buildings, or sharing borehole fields between an office building and an apartment building.

While WA reduces annual net heat extraction from ground more than WW in all scenarios, WW is more effective for reducing total borehole length in all scenarios except the larger AB with the shallow field (Table 5). This is attributed to the stable availability of WW throughout the year in contrast with the seasonality of WA, making the former better matched with heat demand. Similarly, it can be observed that total borehole length is further reduced in active combined scenarios compared to active WA scenarios, even though annual net heat extraction remains nearly unchanged between the two. Therefore, it is indicated that seasonal timing of waste heat utilization influences its effectiveness, since the utilization potentially affects ground temperatures on different timescales: compensation for long-term ground cooling, and for ground cooling occurring during the year, in winter. This also raises the question of the reliability of waste heat availability. In the former case, it is sufficient for the required amount of waste heat to be seasonally available and transferrable to the ground. Since ground heat balance only needs to be maintained on a long timescale, more time is available to react to issues such as misestimated ground heat balance. In contrast, in the latter case, the effectiveness of the waste heat is dependent on its availability during the heating season, and a deviation of the availability from expected during the coldest period of the year

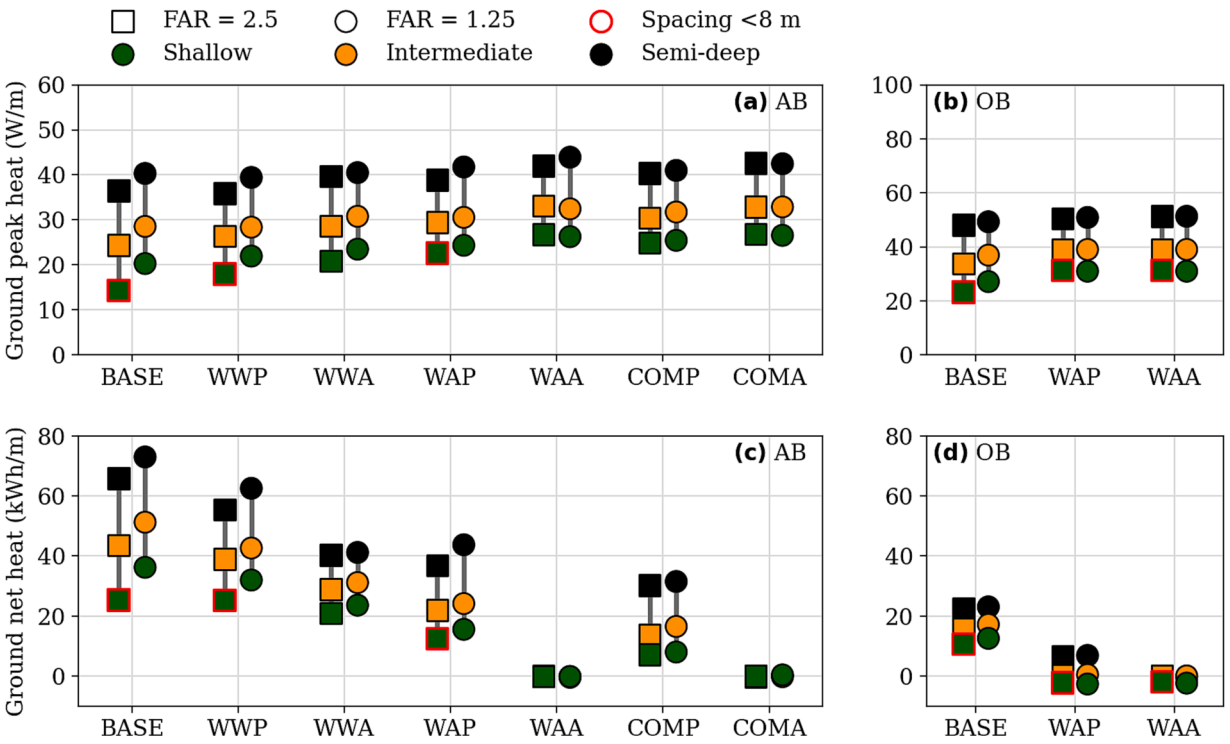

Fig. 6. Peak heat extraction rate (a–b) and annual net heat extraction (c–d) per borehole length for the 50th year of all studied scenarios.

Table 6
Utilized waste heat, utilization rate and matching rate for the 50th year. The results are shown as ranges from shallow to semi-deep field.

Floor-to-area ratio	Building	Scenario	Utilized waste heat (kWh/m^2)	Utilization rate (%)	Matching rate (%)
FAR = 2.5	AB	WWP	11.3–9.7	47.3–40.4	88.2
		WWA	17.3	72.3	88.2
		WAP	25.1–17.6	30.0–21.0	59.0–68.5
		WAA	31.8–31.7	38.0	48.6–48.7
		COMP	31.5–24.0	29.2–22.3	63.9–74.3
		COMA	32.8–32.7	30.5	58.2–56.8
	OB	WAP	20.7–12.6	17.5–10.7	16.8–19.4
		WAA	17.3–15.7	14.6–13.4	18.2–17.0
FAR = 1.25	AB	WWP	10.7–9.2	44.9–38.6	88.1–88.4
		WWA	17.3	72.3	88.2
		WAP	23.5–15.8	28.1–18.9	60.8–70.9
		WAA	32.0–31.9	38.3–38.1	48.6–48.5
		COMP	31.0–23.6	28.8–22.0	64.4–73.6
		COMA	32.9–32.5	30.5–30.2	58.2–56.6
	OB	WAP	21.1–14.4	17.9–12.2	16.7–19.5
		WAA	17.4–15.7	14.8–13.3	18.2–16.9

could lead to excessive cooling of the ground loop and the need to resort to the use of an electric boiler. In addition, compensating for an overestimated waste heat source is more difficult during winter.

As seen in Section 2.2, energy from waste air of the modern buildings is not available during most of the heating season. However, the predictability of the available annual energy is high, as ventilation flow rates and temperature setpoints are pre-designed and generally not influenced by building users. In contrast, the availability of energy from wastewater is dependent on the consumption habits of the building users and can therefore be only estimated, statistically. Previous studies have shown that the shape of the domestic hot water consumption profile remains relatively consistent after exceeding a sufficiently large number of building occupants [48]. However, the assumed demographic of the building inhabitants should be considered, since differences in consumption habits among different demographic groups, such as elderly residents or students, can introduce uncertainties in practice.

3.4. Fluid temperatures and electricity consumption

Utilization of waste heat affects the MFT of a borefield, both on an annual timescale and throughout the system lifetime (50 years). Fig. 7 presents the decrease in annual minimum MFT over system lifetime (a) and first-year hourly MFT (b) for the AB with an intermediate-depth field and high urban density. Over system lifetime, the baseline scenario displays the highest reduction in MFT. In contrast, the change in MFT is nearly zero for the combined active scenario, as annual net zero ground heat balance is achieved. The other scenarios fall in between these extremes depending on the amount of net heat extraction from ground. Overall, the long-term decrease in MFT is higher in shallower fields due to smaller borehole spacing. For the OB, the decrease in MFT is generally lower than for the AB, which is attributable to the lower specific annual net heat extraction.

On an annual scale, waste heat utilization increases the variance in MFT, especially increasing MFT levels during the summer (Fig. 7B). This increase in the variation of MFT is, in addition to injected regeneration heat, attributed to reduction of total borehole length, which leads to higher specific heat injection and extraction rates. Additionally, if the borehole count is reduced, the fluid total flow rate and therefore heat capacity rate is also decreased, leading to higher fluid temperature fluctuation with heat extraction and injection. Across all simulated scenarios, the highest summertime MFT is reached with the semi-deep field and active WA or combined scenario, with the maximum values of 30.9 °C for AB and 35.1 °C for OB.

The change in ground loop fluid temperatures impacts the HP performance (Fig. 8). Higher fluid temperature during the summer increases electricity consumption for cooling, as HP condenser temperature must be increased to reject heat to the ground loop. Conversely, the HP requires less electricity for DHW production during summer since the evaporator temperature is higher. For the AB, HP electricity consumption in the baseline scenarios is 11.9–12.5 kWh/m^2,

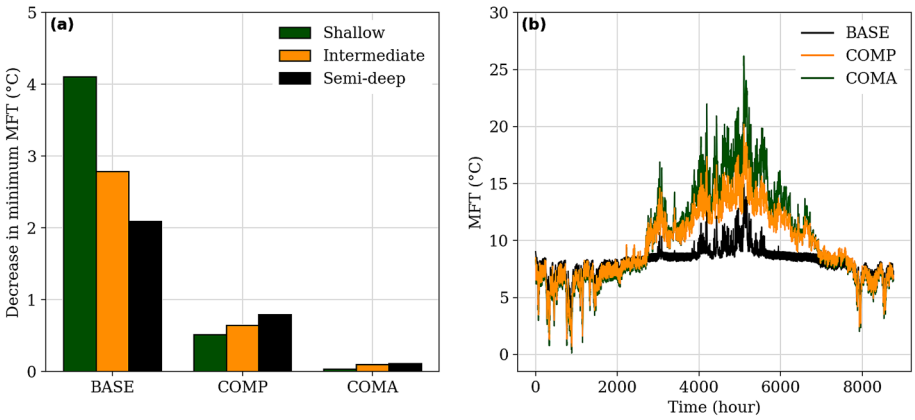

Fig. 7. Decrease in annual minimum MFT over system lifetime (a) and first-year hourly MFT for the AB with an intermediate-depth field (b) with high urban density.

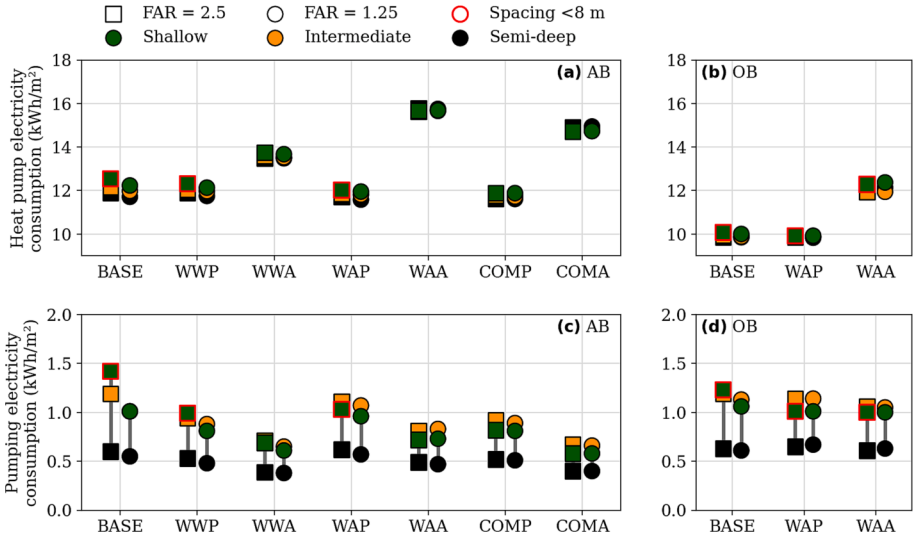

Fig. 8. Heat pump electricity consumption (a–b) and circulation pump electricity consumption (c–d) for the studied scenarios.

increasing with decreased field depth. With passive waste heat utilization, the HP electricity consumption slightly decreases, with the highest decrease (−5.2%) achieved with the shallow field and combined passive waste heat utilization. The decrease indicates that increased COP for DHW production has a larger effect on overall HP electricity consumption than decreased COP for cooling. With active waste heat utilization, HP electricity consumption conversely increases. The increase is due to the utilized waste heat that does not align with building heat demand and is transferred to the ground loop as active regeneration, consuming additional electricity. Notably, active waste heat utilization does not increase the building's peak load on the electricity grid, as the increase in electricity consumption mainly takes place in summer, a period characterized by low electricity demand for heating and high PV production. The annual percentage of directly utilized waste heat that causes no increase in electricity demand is indicated by the matching rate (Table 6).

Circulation pump electricity consumption ranges from 4.6% to 12% of the HP electricity consumption across the baseline scenarios of both building types and sizes. The lowest values are achieved with the semi-deep fields due to lowest total borehole length and total flow rates. Consequently, most of the scenarios with waste heat utilization exhibit reduced pumping electricity consumption, with a higher reduction observed when waste heat utilization has a higher impact on the field dimensions. Despite the decrease in pumping electricity consumption, the increased HP electricity consumption due to regeneration is not offset in any of the active scenarios. Additionally, with passive WA and deeper fields, the pumping electricity consumption can slightly increase, since regeneration heat may need to be transferred to the ground when the ground loop could otherwise be operated at lower flow rate.

3.5. Economic evaluation

In Fig. 9, overview of the economic performance is presented in terms of the levelized cost of heating (LCOH) with different waste heat utilization options. In the AB, the system configurations yield a LCOH range of 124–167 €/MWh, with the best scenario being combined passive waste heat with the shallow field. In the OB, a higher LCOH of 221–273 €/MWh is achieved, with the best scenario being passive WA with the shallow field. At maximum, the inclusion of waste heat utilization in both the AB and the OB results in reduction of LCOH of 13.5% and 7.3%, respectively, when compared to the best baseline scenarios. The cost reduction is slightly lower than the result (20%) of Hirvonen et al. [24], which can be attributed to a more conservative estimation of waste heat availability in this study. Overall, passive waste heat utilization enables slightly lower cost levels compared to active utilization with the reference cost assumptions. Furthermore, the inclusion of waste heat utilization in the larger building version improves the economic feasibility in comparison to the smaller building version due to relatively lower investment costs. The lower investment costs are due to the smaller relative decrease in total borehole length, and the economy of

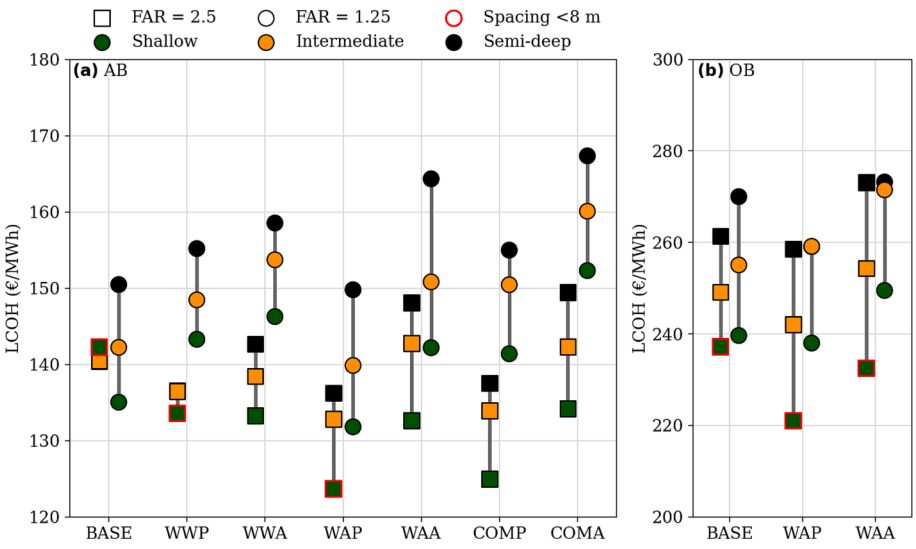

Fig. 9. Comparison of levelized cost of heating (LCOH) for the different scenarios.

scale assumed for the regeneration heat exchangers. Finally, shallow boreholes generally are advantageous economically with waste heat utilization, as indicated by a decreasing trend in LCOH for both the AB and OB.

Due to the lowest LCOH, the larger AB scenarios with the shallow fields are further evaluated in Fig. 10, comparing the cost structures with the baseline scenarios. The annual system cost can be observed to largely consist of three major components: borehole capital expenditure (CAPEX), HP CAPEX, and HP operating expenditure (OPEX). The differences in waste heat utilization costs among the scenarios account for some of the variations depicted in Fig. 9. The cost of the WW regeneration heat exchanger is relatively high, decreasing the feasibility of the WW scenarios. In contrast, the investment costs for WA utilization are relatively low. However, active WA utilization increases the regeneration OPEX in comparison to passive WA utilization, as a large part of heat is used for ground regeneration rather than for directly covering the heat demand, indicated earlier by the lower matching rates. For the AB, the increased OPEX is partially offset by the decreased borehole CAPEX, as active utilization reduces the borehole count. Further benefit could be achieved with variable electricity pricing, as the increased electricity consumption mainly takes place during summer, aligning with expectedly low electricity prices. For the OB, the borehole count and total length generally remain constant, providing no compensation for the increased OPEX. This trend is consistent across all the scenarios with the

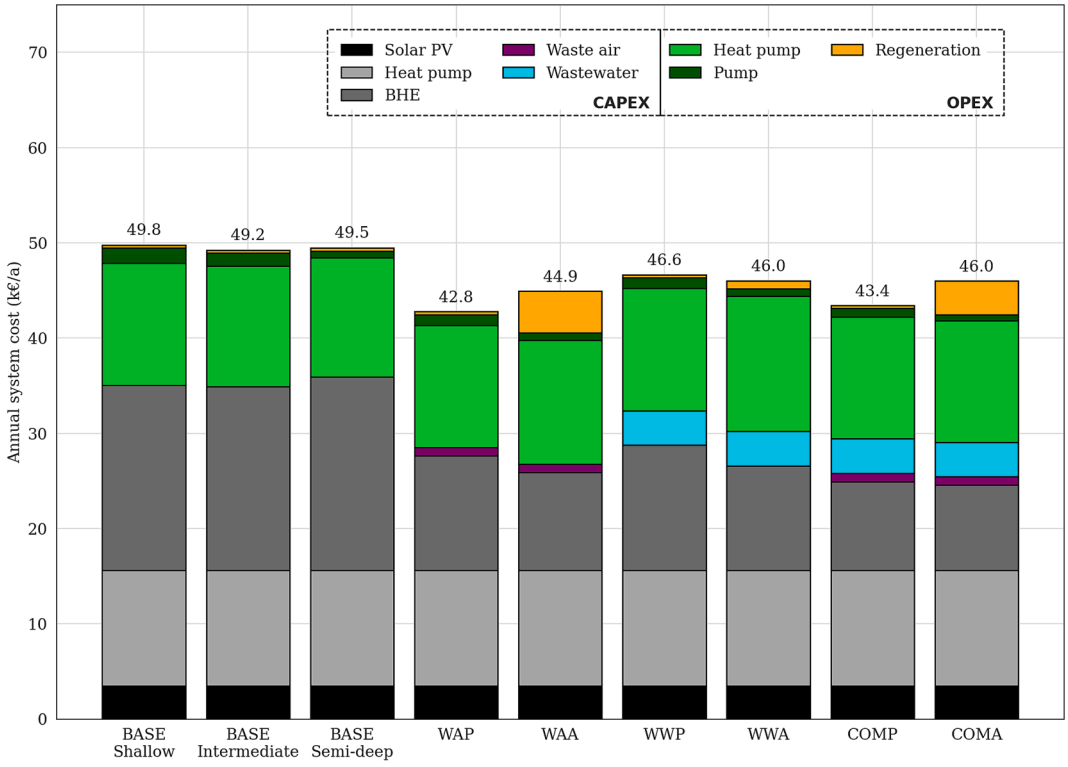

Fig. 10. Cost breakdown of selected scenarios: baseline scenarios compared to scenarios with waste heat utilization with shallow field for the larger AB. Total annual system cost shown above the bars.

reference electricity price. The capital expenditure for HP and solar PV remains constant in the studied scenarios and is included for scale purposes.

Based on the previous analysis, it can be deducted that the results and comparative performance of the scenarios are dependent on the price of electricity. To extend the economic analysis beyond the reference electricity price (15 c/kWh), the scenarios were simulated with an extended electricity price range of (5–40 c/kWh). For each scenario, the LCOH is compared to that of a reference district heating system. A break-even electricity price is determined as the price at which the GSHP system reaches an equal LCOH with the district heating system. For the OB, the reference LCOH is 171 €/MWh (high urban density) and 181 €/MWh (moderate urban density). The GSHP scenarios exhibit higher LCOH, and regardless of the borefield configuration or floor area ratio, do not break even with the lowest electricity price. For the AB, break-even is achieved. The reference LCOH is 143 €/MWh (high urban density) and 150 €/MWh (moderate urban density). Fig. 11 illustrates that the break-even point strongly depends on the regeneration type and floor area ratio, aligning with the earlier assessment of LCOH. A higher price level (ca. 27.5 c/kWh) would be acceptable for achieving break-even for the AB. The semi-deep fields demonstrate improved resilience to electricity price due to the higher cost reduction in borehole investment, allowing for a higher electricity price compared to deeper fields. Similarly, with waste heat utilization, a higher electricity cost level would be acceptable for compared to active utilization due to the increased electricity consumption for regeneration, particularly evident with waste air (27.5 c/kWh vs. 22.5 c/kWh). Lastly, with a higher floor area ratio, the sensitivity to electricity price is lower while the improvement to baseline is more significant.

4. Conclusions

The analysis conducted in this study examined the effect of waste heat regeneration on borehole field sizing for modern office and apartment buildings in Finland. Three options for waste heat utilization (wastewater, waste air, and their combination) were compared in terms of techno-economic performance, considering both passive (heat directly to ground loop) and active (heat to heat pump evaporator) versions. An iterative model was developed to calculate the hourly heat balances of a ground source heat pump system over a simulation period of 50 years, utilizing g-functions. Circular-shaped fields were iteratively dimensioned for 60 scenarios, which encompassed different waste heat utilization options, varying borehole depths, and two floor-to-area ratios representing typical densely built and moderately dense urban districts. Based on the technical and economic findings, the following conclusions can be drawn:

1. The utilization of commonly available waste heat from waste air or wastewater can enable GSHP systems in densely built areas, addressing space limitations. Waste heat utilization enabled the use of a shallow borefield for the apartment building by reducing the borehole count to meet the minimum spacing requirement of 8 m, serving as an alternative to increasing borehole depth. Overall, the highest reduction in total borehole length (54% for the apartment building and 26% for the office building) was achieved with waste heat utilization in shallow fields (higher density and poorer baseline performance) and larger buildings. Notably, active waste heat utilization consistently outperformed passive utilization in reducing borehole length for the apartment building (27% vs. 21% on average). However, in the office building, the further benefit of active utilization was only marginal, as passive utilization could already achieve an annual net zero ground heat balance. The significant decrease in total borehole length enables a notable reduction in upfront investment costs, which are a key barrier to the implementation of GSHP systems.
2. Seasonal profiles of waste heat availability and building heat demand should be considered when integrating waste heat to a GSHP system. Waste heat is more valuable during the heating season, compensating for heat extraction from ground and influencing the lowest fluid temperatures during winter. Consequently, wastewater utilization resulted in a higher average reduction in borehole length compared to waste air (passive: 18% vs. 14%, active: 27% vs. 22%), despite the greater annual energy utilization from waste air in all scenarios. However, in the only scenario requiring waste heat

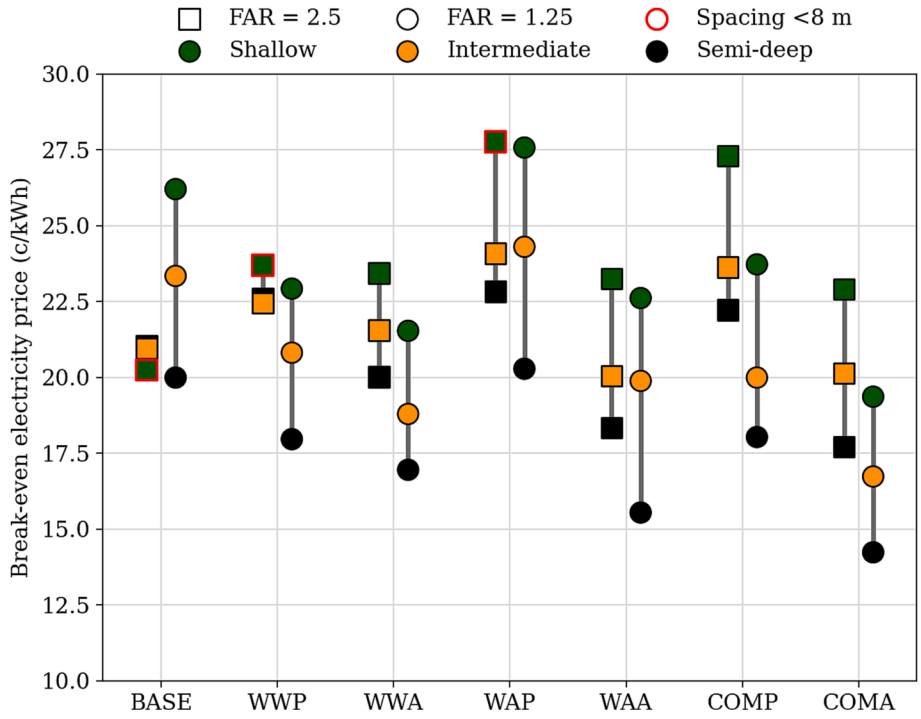

Fig. 11. Break-even electricity price for the different scenarios in the apartment building in comparison to a reference district heating and cooling investment.

utilization to achieve the minimum borehole spacing, the effect of waste air was more significant (passive: 37% vs. 31%, active 46% vs. 43%). Furthermore, waste air was found more effective for borehole fields with high energy demand rather than high peak heat demand, as shown by higher maximum borehole length reduction for the apartment building (46%) compared to the office building (26%).

3. Waste heat utilization can effectively reduce the levelized cost of heating (LCOH) in GSHP systems. Consistent with the technical findings, shallow fields and larger buildings exhibit lower LCOH due to the combination of substantial borehole depth reduction and lower specific cost of utilized waste heat. The maximum reduction in LCOH reached 13.5% (apartment building) and 7.3% (office building) compared to baseline. While wastewater utilization enabled a higher average reduction in total borehole length, waste air utilization was found to enable a lower LCOH due to lower investment costs. Additionally, passive utilization was found economically more favorable than active utilization due to the associated net electricity consumption, which was decreased by passive utilization (up to 5%) but increased by active utilization (10–30%) and therefore not fully compensated by the achieved reduction in total borehole length. As a result, passive utilization demonstrated greater resilience to higher electricity prices and would better ensure feasibility compared to district heating.

Further studies are needed to improve the cost-effectiveness of active waste heat utilization, focusing on short-term and long-term control strategies. In this study, the operation was based on a simplistic approach of utilizing available waste heat whenever it was available, without considering factors such as current heating and cooling demands, own electricity production, or variable electricity price. Regarding field dimensioning, limitations in field shape could be considered in the analysis. For example, in practice, drilling may need to be focused on the edges of the plot area. Additionally, exploring the potential of shared fields between buildings could maximize the benefits from different waste heat availability profiles across various building types or other nearby waste heat sources, such as cooling processes of grocery stores and data centers through local low-temperature heating networks. The availability of wastewater heat during winter is critical when system dimensioning relies on it. Modelling methods, such as presented in this study, can be combined with statistical analysis and practical experience from existing installations to estimate safe dimensioning limits and assess the impact of potential variations in wastewater energy availability.

Funding

This work was funded by Business Finland in the project HYBGEO (Hybrid Geothermal Technology and Data Enabling Positive Energy Buildings).

CRediT authorship contribution statement

Andrei Wallin: Conceptualization, Methodology, Software, Formal analysis, Investigation, Data curation, Writing – original draft. **Tomi Thomasson:** Methodology, Software, Formal analysis, Investigation, Data curation, Writing – original draft, Visualization. **Rinat Abdurafikov:** Conceptualization, Validation, Writing – review & editing, Supervision, Project administration.

Declaration of Competing Interest

The authors declare that they have no known competing financial interests or personal relationships that could have appeared to influence the work reported in this paper.

Data availability

Data will be made available on request.

Acknowledgments

The authors thank the partners in the project consortium for their collaboration and the valuable technical insights.

References

[1] L. Rybach, Geothermal heat pump production sustainability—The basis of the Swiss GHP Success Story, Energies (Basel) 15 (21) (2022) 7870, https://doi.org/10.3390/en15217870.
[2] REPowerEU Plan. Brussels: European Commission, 2022.
[3] C. Song, Y. Li, T. Rajeh, L. Ma, J. Zhao, W. Li, Application and development of ground source heat pump technology in China, Protection and Control of Modern Power Systems 6 (1) (2021) 17, https://doi.org/10.1186/s41601-021-00195-x.
[4] H. Sadeghi, A. Ijaz, R.M. Singh, Current status of heat pumps in Norway and analysis of their performance and payback time, Sustainable Energy Technol. Assess. 54 (2022), 102829, https://doi.org/10.1016/j.seta.2022.102829.
[5] A. Ramos-Escudero, M. García-Cascales, Barriers behind the retarded shallow geothermal deployment in specific areas: A comparative case study between Southern Spain and Germany, Energies (Basel) 15 (13) (2022) 4596, https://doi.org/10.3390/en15134596.
[6] Lauttamäki, V., Ground-source heat on facilities' heating market in Finland from the times of energy crisis in the 1970s until 2030, Doctoral thesis, University of Turku, Turku, 2018.
[7] L. Cassina, L. Laloui, A.F. Rotta Loria, Thermal interactions among vertical geothermal borehole fields, Renew. Energy 194 (2022) 1204–1220.
[8] D. Romanov, B. Leiss, Geothermal energy at different depths for district heating and cooling of existing and future building stock, Renew. Sustain. Energy Rev. 167 (2022), 112727, https://doi.org/10.1016/j.rser.2022.112727.
[9] K. Huchtemann, D. Müller, Combined simulation of a deep ground source heat exchanger and an office building, Build Environ 73 (2014) 97–105, https://doi.org/10.1016/j.buildenv.2013.12.003.
[10] K. Jiao, C. Sun, R. Yang, B.o. Yu, B. Bai, Long-term heat transfer analysis of deep coaxial borehole heat exchangers via an improved analytical model, Appl. Therm. Eng. 197 (2021) 117370, https://doi.org/10.1016/j.applthermaleng.2021.117370.
[11] Poratek, Energiakaivot, 2023. [Online]. Available: https://www.poratek.fi/energiakaivot/.
[12] H. Li, J. Hou, T. Hong, Y. Ding, N. Nord, Energy, economic, and environmental analysis of integration of thermal energy storage into district heating systems using waste heat from data centres, Energy 219 (2021) 119582, https://doi.org/10.1016/j.energy.2020.119582.
[13] F. Guo, X. Zhu, P. Li, X. Yang, Low-grade industrial waste heat utilization in urban district heating: Simulation-based performance assessment of a seasonal thermal energy storage system, Energy 239 (2022) 122345, https://doi.org/10.1016/j.energy.2021.122345.
[14] S.E.A. Gehlin, J.D. Spitler, Long-term performance monitoring of GSHP systems for commercial, institutional, and multi-family buildings, (2022).
[15] H. Hemmatabady, B. Welsch, J. Formhals, I. Sass, AI-based enviro-economic optimization of solar-coupled and standalone geothermal systems for heating and cooling, Appl. Energy 311 (2022) 118652, https://doi.org/10.1016/j.apenergy.2022.118652.
[16] J. Hirvonen, K. Sirén, A novel fully electrified solar heating system with a high renewable fraction - Optimal designs for a high latitude community, Renew Energy 127 (2018) 298–309, https://doi.org/10.1016/j.renene.2018.04.028.
[17] J. Hirvonen, H. ur Rehman, K. Sirén, Techno-economic optimization and analysis of a high latitude solar district heating system with seasonal storage, considering different community sizes, Sol. Energy 162 (2018) 472–488.
[18] K. Allaerts, M. Coomans, R. Salenbien, Hybrid ground-source heat pump system with active air source regeneration, Energy Convers. Manag. 90 (2015) 230–237, https://doi.org/10.1016/j.enconman.2014.11.009.
[19] A. Walch, N. Mohajeri, A. Gudmundsson, J.L. Scartezzini, Quantifying the technical geothermal potential from shallow borehole heat exchangers at regional scale, Renew. Energy 165 (2021) 369–380, https://doi.org/10.1016/j.renene.2020.11.019.
[20] A.R. Puttige, S. Andersson, R. Östin, T. Olofsson, Modeling and optimization of hybrid ground source heat pump with district heating and cooling, Energy Build. 264 (2022) 112065, https://doi.org/10.1016/j.enbuild.2022.112065.
[21] Eurostat, Cooling and heating degree days by country - annual data, 2023. [Online]. Available: https://ec.europa.eu/eurostat/web/products-datasets/-/nrg_chdd_a.
[22] S. Guillén-Lambea, B. Rodríguez-Soria, J.M. Marín, Evaluation of the potential energy recovery for ventilation air in dwellings in the South of Europe, Energy Build 128 (2016) 384–393, https://doi.org/10.1016/j.enbuild.2016.07.011.
[23] Ministry of the Environment, D2 Suomen Rakennusmääräyskokoelma: Rakennusten sisäilmasto ja ilmanvaihto. 2002.
[24] J. Hirvonen, J. Jokisalo, R. Kosonen, J. Kurnitski, M. Thalfeldt, Seasonal storage of residential exhaust air and sewage waste heat, E3S Web Conf. 246 (2021) 06009, https://doi.org/10.1051/e3sconf/202124606009.

[25] Equa, IDA Indoor Climate and Energy 4, Quality, 2009. [Online]. Available: http://www.equa.se/dncenter/Brochure_IDA_ICE 4.0_web_v4.pdf.
[26] Jylhä, K. et al., Rakennusten energialaskennan testivuosi 2012 ja arviot ilmastonmuutoksen vaikutuksista, 2012.
[27] Jalkanen, R., Kajaste, T., Kauppinen, T., Pakkala, P., and Rosengren, C., Kaupunkisuunnittelu ja asuminen. 2017.
[28] Ecowec, Ecowec B10, 2023. [Online]. Available: https://ecowec.com/tuotteet/ecowec-b10/.
[29] J. Wallin, Case studies of four installed wastewater heat recovery systems in Sweden, Case Stud. Therm. Eng. 26 (2021) 101108, https://doi.org/10.1016/j.csite.2021.101108.
[30] A. Laitinen, A. Wallin, Jäteveden lämmöntalteenoton energiatase kaupungissa. VTT Research Report VTT-R-00582-22., (2022).
[31] C. Wärff, M. Arnell, R. Sehlén, U. Jeppsson, Modelling heat recovery potential from household wastewater, Water Sci. Technol., 81(8) (2020)1597–1605, https://doi.org/10.2166/wst.2020.103.
[32] Oikeusministeriö, Ympäristöministeriön asetus uuden rakennuksen energiatehokkuudesta, Suomen säädöskokoelma, 2017. [Online]. Available: http://www.finlex.fi/data/normit/37188/D3-2012_Suomi.pdf.
[33] M. Cimmino, J. Cook, pygfunction 2.2: New features and improvements in accuracy and computational efficiency, (2022), https://doi.org/10.22488/okstate.22.000015.
[34] Y. Brussieux, M. Bernier, A hybrid model for generating short-time g-functions, (2018), 1–9, https://doi.org/10.22488/okstate.18.000011.
[35] P. Mogensen, Fluid to duct wall heat transfer in duct system heat storages, in Document - Swedish Council for Building Research, (pt 2) (1983) 652–657.
[36] T. Thomasson, R. Abdurafikov, Dynamic simulation and techno-economic optimization of deep coaxial borehole heat exchangers in a building energy system, Energy Build. 275 (2022) 112457, https://doi.org/10.1016/j.enbuild.2022.112457.
[37] Y. Luo, J. Yu, T. Yan, L. Zhang, X. Liu, Improved analytical modeling and system performance evaluation of deep coaxial borehole heat exchanger with segmented finite cylinder-source method, Energy Build. 212 (2020) 109829, https://doi.org/10.1016/j.enbuild.2020.109829.
[38] P. Bayer, M. de Paly, M. Beck, Strategic optimization of borehole heat exchanger field for seasonal geothermal heating and cooling, Appl. Energy 136 (2014) 445–453, https://doi.org/10.1016/j.apenergy.2014.09.029.
[39] W. Mazzotti, A. Lazzarotto, J. Acuña, P. Björn, Deep Boreholes for Ground-Source Heat Pump, (2018).
[40] H. Skarphagen, D. Banks, B.S. Frengstad, H. Gether, Design considerations for borehole thermal energy storage (BTES): A review with emphasis on convective heat transfer, Geofluids 2019 (2019) 1–26, https://doi.org/10.1155/2019/4961781.
[41] H. Holmberg, J. Acuña, E. Næss, O.K. Sønju, Thermal evaluation of coaxial deep borehole heat exchangers, Renew. Energy 97 (2016) 65–76, https://doi.org/10.1016/j.renene.2016.05.048.
[42] D. Sveinbjörnsson, L. Laurberg Jensen, D. Trier, I. Ben Hassine, X. Jobard, FLEXYNETS D2.3 - Large Storage Systems for DHC Network, (2019).
[43] Y. Haahtela, J. Kiiras, Building Construction Cost Data 2013 [Talonrakennuksen kustannustieto 2013], (2013).
[44] Ecowec, Ecowec B8, 2023. [Online]. Available: https://ecowec.com/tuotteet/ecowec-b8/.
[45] M.A. Tribe, R.L.W. Alpine, Scale economies and the “0.6 rule”, Eng. Costs Prod. Econ’. 10 (1) (1986) 271–278.
[46] Helen, District heat prices, 2023. [Online]. Available: https://www.helen.fi/en/heating-and-cooling/district-heat/district-heat-prices.
[47] Fortum and VTT, Apros, 2023. [Online]. Available: www.apros.fi/.
[48] K. Ahmed, P. Pylsy, J. Kurnitski, Hourly consumption profiles of domestic hot water for different occupant groups in dwellings, Sol. Energy 137 (2016) 516–530, https://doi.org/10.1016/j.solener.2016.08.033.